

See discussions, stats, and author profiles for this publication at: <https://www.researchgate.net/publication/256682420>

# Positron annihilation studies on the phase transition of benzene and reactivity of nitrobenzene in confined framework of ZSM-5 zeolite

ARTICLE *in* CHEMICAL PHYSICS LETTERS · DECEMBER 2006

Impact Factor: 1.9 · DOI: 10.1016/j.cplett.2006.10.062

---

CITATIONS

10

---

READS

27

3 AUTHORS, INCLUDING:



**Dhanadeep Dutta**

Bhabha Atomic Research Centre

56 PUBLICATIONS 381 CITATIONS

SEE PROFILE



**P. K. Pujari**

Bhabha Atomic Research Centre

154 PUBLICATIONS 632 CITATIONS

SEE PROFILE

# Positron annihilation studies on the phase transition of benzene and reactivity of nitrobenzene in confined framework of ZSM-5 zeolite

D. Dutta, A. Sachdeva, P.K. Pujari \*

*Radiochemistry Division, Bhabha Atomic Research Centre, Mumbai 400 085, India*

Received 23 June 2006; in final form 16 October 2006

Available online 20 October 2006

## Abstract

We present a new result on positron annihilation spectroscopy on phase transition and reactivity (towards positronium) of confined liquids in the pores of ZSM-5 zeolite using Doppler broadened annihilation radiation measurement and lifetime spectroscopy. Benzene confined in intergranular spaces (mesopores) and micropores in ZSM-5 shows two distinct freezing points. While the freezing temperature of benzene in mesopore is close to the bulk value, a 5–6 K depression is observed for benzene inside micropores (size  $\sim 5$  Å). The reactivity of nitrobenzene towards positronium is studied in nitrobenzene–benzene mixture incorporated in ZSM-5 pores. An anomalous enhancement in the reactivity is observed as compared to measurements in the bulk liquid. The results are discussed.

© 2006 Elsevier B.V. All rights reserved.

## 1. Introduction

The physical and chemical behavior of liquids and solids confined in micro pores has attracted considerable attention in recent years. This is due to the fundamental interest behind the combined effects of finite size, surface forces, surface anisotropy, pore disorder and reduced dimensionality on the properties of solids and liquids. Also, the properties of liquids in micropores have potential applications in catalysis, membrane separations, interfacial adhesion and lubrication [1], fabrication of nano particles in micropore templates and in many other areas [2–5]. In this context freezing and melting behavior of molecules confined in silica pores have been studied using a variety of techniques such as Differential Scanning Calorimetry [6,7], Nuclear Magnetic Resonance [7], Dielectric Spectroscopy [8]. The crystallization behavior of confined fluid and their dependence on the pore size have also been studied by computer simulation [8–10].

These studies have explored the effect of pore structure and interaction of confined molecules with pore wall on

their freezing and melting behavior. Despite complexities due to multiple effect such as geometry, size and surface properties, these studies reveal that the freezing and melting temperature of the liquid inside the pores increases when the interaction potential between the pore wall and the liquid is more attractive as compared to the interaction potential that would result if the pore walls were to be made up of solid phase of the confined molecules. Similarly, the freezing temperature decreases for ‘weakly attractive’ or ‘repulsive’ pore wall.

Positron annihilation spectroscopy, an *in situ*, nondestructive technique is a sensitive micro probe to study the behavior of liquids/solids in confined geometry. Several studies using this technique on the phase transition (freezing and melting) behavior of gases ( $\text{CO}_2$ ,  $\text{N}_2$ ) in microporous solids have been reported [11–15]. In porous material a substantial fraction of thermalized positron may form positronium (a bound state of an electron and positron) at the bulk-pore interface that diffuses and localises in cavities or regions of low electron density. Positronium (Ps) may exist in two states, viz., *para*-positronium (*p*-Ps) and *ortho*-positronium (*o*-Ps) formed at a ratio of 1:3. Intrinsically *p*-Ps annihilates into two photons with a lifetime of 0.125 ns, while *o*-Ps decays into three photons

\* Corresponding author.

E-mail address: [pujari@magnum.barc.ernet.in](mailto:pujari@magnum.barc.ernet.in) (P.K. Pujari).

with a much larger lifetime of 140 ns. However, in the presence of matter *o*-Ps can decay into two photons through a process known as pick-off annihilation, whereby the positron in *o*-Ps seeks out electrons from the pore surface with opposite spin and annihilates through the two-photon mode. This pick-off decay characteristic of *o*-Ps is of great utility, enabling its use as a microprobe in the study of molecular materials [16]. The trapped *o*-Ps inside the micropore (parametrized on the average as a spherical hollow region of radius  $R$ ) has a probability of being found in and about the cavity given by the square modulus of its wave function  $\Psi_{Ps}(r)$  with  $r$  measured from the center of the cavity. The pick-off annihilation rate (inverse of pick-off lifetime) is given as

$$\lambda_p = 4\pi r_0^2 c Z_{\text{eff}} \int_0^\infty |\Psi_{Ps}(r)|^2 \rho(r) d^3r, \quad (1)$$

where  $r_0 (= e^2/m_0c^2)$ ,  $e$  being electronic charge and  $m_0$  being its rest mass) is the classical electron radius,  $\rho(r)$  is the number density of atoms around the cavity and  $Z_{\text{eff}}$  is the available number of valence electrons per atom contributing to the process. This model [17] has been further developed and a simple relationship between the pick-off lifetime ( $\tau_p$ ) and micro cavity radius ( $R \leq 10 \text{ \AA}$ ) is obtained as [18]

$$\tau_p = 1.88R - 5.07, \quad (2)$$

where  $\tau_p$  is in ns and  $R$  is in  $\text{\AA}$ . For larger pores (pore radius  $R > 10 \text{ \AA}$ ) the contribution of *o*-Ps intrinsic annihilation (three gamma) becomes significant along with *o*-Ps pick-off annihilation; hence the lifetime becomes larger and the annihilation rate is given by

$$\lambda = \lambda_p + \lambda_{3\gamma} = \zeta \left( \frac{\delta}{R'} \right) + \lambda_{3\gamma}, \quad (3)$$

where,  $\lambda_{3\gamma} (= 1/140 \text{ ns}^{-1})$  is the intrinsic  $3\gamma$  annihilation rate of *o*-Ps [19]. It is however imperative that  $\zeta$  includes the parameters such as  $Z_{\text{eff}}$  (effective number of valence electrons available from surrounding atom) as well as the density ( $\rho < 1$ ) of the porous material.  $R'$  is the size parameter for the large pore and  $\delta$  is the diffusivity parameter at the surface of the mesopore. The total annihilation rate, however, does not depend on the geometric shape of the pore [19,20] and the calibration evolved ( $\lambda = 0.3/R' + 1/140$ ) has worked well for all calculable data on silica and zeolite materials [19,21].

As mentioned earlier, a number of positron annihilation spectroscopic studies have been carried out to understand the freezing and melting behavior of gases in confined geometry. These include temperature dependent studies on  $\text{CO}_2$  confined in vycor glass [11], where in a systematic response of positron/positronium is seen at temperatures corresponding to phase transition. Hysteresis in cooling and heating cycle has also been observed in number of cases, which is attributed to the mechanism of pore melting/freezing [12–14]. In addition, capillary condensation phenomena of nitrogen gas in mesopores [15] has been studied using this technique.

However, positron annihilation studies in confined liquids in terms of its phase transition behavior as well as interaction mechanism of positronium with liquids confined in small pores have not been reported so far. In the present work, freezing and melting behavior of benzene confined in ZSM-5 zeolite has been studied using positron lifetime and Doppler broadened annihilation radiation measurement. The reactivity of nitrobenzene towards positronium is also investigated using positron lifetime spectroscopy by systematically varying the concentration of nitrobenzene in nitrobenzene–benzene mixture. The objective of the work has been to study the phase transition (freezing behavior) of benzene as well as the reactivity of Ps with known quencher (nitrobenzene) in confined geometry.

## 2. Experimental

Commercially available ZSM-5 zeolite ( $\text{SiO}_2/\text{Al}_2\text{O}_3 = 30$ , surface area  $380 \text{ m}^2 \text{ gm}^{-1}$  and pore volume  $0.22 \text{ cm}^3 \text{ gm}^{-1}$ ), analytical grade benzene and nitrobenzene were used for the present study. ZSM-5 has a porous network system, which belongs to pentasil family where ten oxygen rings with connecting Si or Al atoms make the high internal surface of the pore [22]. The zeolite sample was heated at 573 K under vacuum for 7–8 h to remove adsorbed air and moisture. It was cooled to room temperature and appropriate volume of benzene or its mixture with nitrobenzene, as the case may be, was injected into the sample (in vacuum) with a syringe. The liquid-sample mixture was kept overnight and heated at 323 K for homogeneous adsorption of liquid into the pores. The sample was evacuated at room temperature for appropriate time to remove the liquid /vapor at bulk surface of the sample. FTIR measurements were carried out using JASCO FTIR-610 instrument for confirming the incorporation of benzene. It exhibited peaks at 3041, 3074 and  $3095 \text{ cm}^{-1}$  (C–C, C–H stretching vibration of  $\text{C}_6\text{H}_6$ ) confirming the incorporation of benzene in to the micro pores of zeolite (Fig. 1). Thermogravimetric (TGA) measurements also confirmed the incorporation of benzene in the zeolite matrix.

For low temperature measurements, the sample along with the source ( $\sim 8 \mu \text{ Ci}$  deposited on thin nickel foil) was mounted on the cold head of an APD closed cycle helium refrigerator. Temperature variation was carried out in 1 K interval with an accuracy of 0.01 K. Doppler broadened annihilation radiation measurements were carried out using a HPGe detector having resolution of 1.7 keV at 1332 keV photo peak of  $^{60}\text{Co}$ . The shape parameter, namely, S-parameter defined as the normalized integrated counts in the energy range  $511 \pm 1 \text{ keV}$  was evaluated.

Positron annihilation lifetime measurements were carried out using plastic scintillation detectors in a fast–fast coincidence system. The resolving time (fwhm) measured with a  $^{60}\text{Co}$  source was 300 ps for the positron window

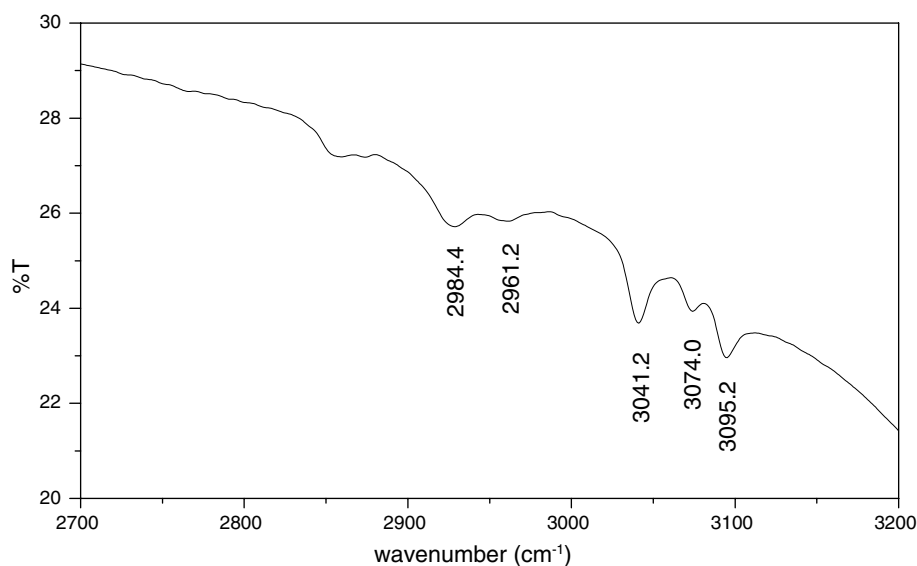


Fig. 1. FTIR spectra of benzene inside the pores of ZSM-5 zeolite sample.

settings, with a time constant of 25 ps per channel. Data analysis was carried out using PATFIT program [23].

For the studies on the reactivity of benzene–nitrobenzene mixture on positronium, the sample along with the source was put in a cylindrical glass tube. Lifetime measurements were carried out on samples containing nitrobenzene–benzene mixture in which the concentration of nitrobenzene was varied from 0.001 to 1.1 mmol.

### 3. Results and Discussion

Positron annihilation lifetime results (room temperature) in ZSM-5 zeolite before and after the incorporation of benzene inside the porous network is shown in Table 1. The two distinct long-lived components (labeled  $\tau_3$  and  $\tau_4$ ) in pure ZSM-5 sample correspond to *o*-Ps annihilation in microcavities within the grains and in intergranular mesoscopic pores, respectively. The corresponding pore radii, calculated using Eqs. (2) and (3), reveal the pore dimensions to be 5 and 13 Å respectively (Table 1). When benzene molecules are incorporated into the zeolite matrix, they localize in micro and mesopores. After incorporation of benzene in this matrix, only one long-lived component of *o*-Ps is obtained (referred to as  $\tau_3$ ) which originates from benzene present in the micro and mesopores. The life-time (2.8 ns) is, however, smaller than that obtained in bulk liquid benzene (3.1 ns) [16].

#### 3.1. Phase transition

In order to monitor the changes associated with freezing of benzene in pores of ZSM-5 at nanoscopic scale, Doppler Broadening measurements were carried out from 300 K to 150 K. In addition, Positron lifetime measurements were carried out from 282 K to 268 K. Doppler broadened S-parameter for cooling and heating cycles is shown in Fig. 2a and b, respectively. The pick-off lifetime of *o*-Ps and its intensity with temperature during cooling cycle is shown in Fig. 3a and b, respectively. Measured S-parameter shows two distinct discontinuities on cooling around 276–277 K and 272–273 K (Fig. 2a). In the heating cycle too, these two transitions are apparent (Fig. 2b). These two transitions can be ascribed to freezing of benzene in the mesopores and micropores, respectively. The S-parameter data from 265 K at least up to 150 K does not show any fluctuation and, therefore, not shown in the Fig. 2a and b. For a porous medium with an average pore size that is much greater than the size of the fluid molecules, the shift in melting point is described by well-known Gibbs–Thomson equation

$$T_{m(\text{bulk})} - T_m(r_p) = \frac{2V_m T_{m(\text{bulk})}(\gamma_{lw} - \gamma_{cw})}{r_p \Delta H_m}, \quad (4)$$

where  $\gamma_{cw}$  and  $\gamma_{lw}$  are respectively the crystal-wall and liquid-wall interaction energy,  $T_{m(\text{bulk})}$  is the bulk melting point,  $r_p$  is the pore radius,  $V_m$  is the crystal molar volume and  $\Delta H_m$  is the molar melting enthalpy of the crystal [7].

Table 1  
Positron annihilation lifetime in pure and benzene loaded ZSM-5 zeolite

Samples	$\tau_1$ (ns)	$I_1$ (%)	$\tau_2$ (ns)	$I_2$ (%)	$\tau_3$ (ns)	$I_3$ (%)	$R$ (Å) (Eq. (2))	$\tau_4$ (ns)	$I_4$ (%)	$R'$ (Å) (Eq. (3))
ZSM-5	0.22	36.26	0.60	58.56	4.53	3.85	5.11	33.36	1.32	13.14
Benzene loaded ZSM-5	0.20	44.08	0.54	29.45	2.81	26.48	4.19	–	–	–

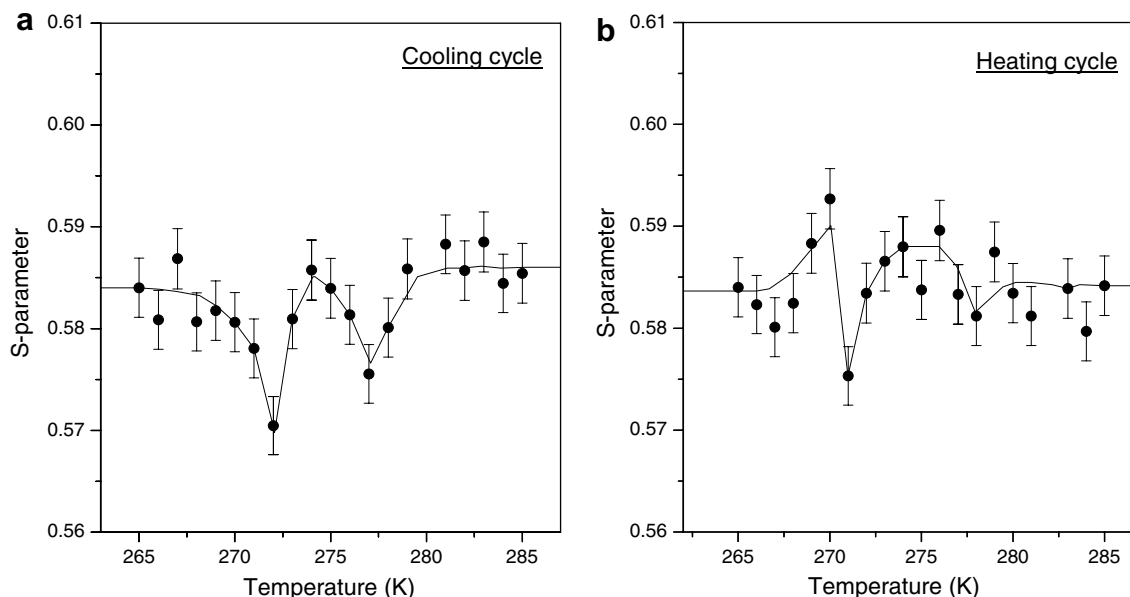


Fig. 2. Temperature dependence of S-parameter during (a) cooling cycle and (b) heating cycle.

The depression in freezing/melting temperature follows the above-mentioned Gibbs–Thomson equation for the mesopore size larger than 60–70 Å [1,10]. So, the Gibbs–Thomson equation is not applicable for determining depression in freezing/melting temperature in mesopores of ZSM-5 (mesopore size 13 Å). Rather, the pore surface anisotropy that determines the strength of liquid-wall interaction and the effect of inhomogeneity of the benzene structure in the confined space are important in determining the shift in freezing point.

The Ps lifetime (Fig. 3a) decreases systematically on cooling from 282 K, which can be ascribed to increase in density of benzene leading to higher pick-off annihilation rate. At  $\sim 276$  K, region of first transition, there is a sharp decrease in lifetime up to 274 K. At  $\sim 273$  K, region of second transition, a discontinuity in lifetime is seen that is considerably higher and decreases monotonically upon cooling at least up to 270 K. The intensity profile (Fig. 3b) too shows changes corresponding to the transition temperature i.e.  $\sim 276$  K and  $\sim 273$  K.

The S-parameter profile is expected to reflect the Ps intensity since it indexes the *p*-Ps having a low momentum spread. Upon cooling, the intensity is seen to decrease reaching a minimum in the region of first transition  $\sim 276$  K followed by an increase up to 274 K. This is similar to the S-parameter response across the first transition (Fig. 2a). On further cooling, there is a sudden drop in intensity at  $\sim 273$  K that corresponds to the second transition (micropore freezing), similar to a minimum seen in S-parameter at  $\sim 272$  K.

With lowering of temperature, the density of benzene in the pores is increased. This reduces the Ps formation probability and consequently intensity reduces. The lifetime of Ps is also expected to decrease because higher density of benzene would enhance the pick-off processes at meso

and micropores. At the onset of first transition i.e.  $\sim 276$  K, lifetime undergoes a sharp decrease up to 274 K. This enhancement of annihilation rate can be ascribed to the freezing of benzene in mesopores. Freezing would lead to a reduction in the volume of the confined benzene leading to creation of free-volume between the pore wall and the frozen benzene surface [11]. This should have been reflected as an increase in the lifetime contrary to what is seen in the present case. On the other hand an increase in intensity of *o*-Ps is seen that is consistent with increase in the surface area of benzene. This could be due to formation of solid particles of benzene. Another possibility is that the freezing is not complete leading to solid–liquid mixtures with large interfaces in this temperature region. At  $\sim 273$  K, there is a discontinuity in lifetime as well as intensity, which can be ascribed to transition in the micropores. The sharp increase in lifetime is due to creation of free-volume upon freezing as discussed earlier. The drop in intensity is in sharp contrast to what is observed at  $\sim 276$  K corresponding to mesopore freezing. This points to a significant difference in the nature of freezing at the mesopore and micropore. The decrease in intensity at  $\sim 273$  K could be due to complete disappearance of liquid surface of benzene. It may be mentioned that Dossch et al. [7] and Bartkowiak et al. [8] have reported orientationally disordered solid phase of benzene molecules. After the formation of this phase at  $\sim 273$  K, we have not observed any other phase transition at least up to 150 K from Doppler broadened annihilation radiation measurement. Also, no remarkable differences in the heating and cooling cycle is seen (Fig. 2a and b).

Dossch et al. [7] have systematically studied the thermal properties of benzene inside MCM-41 and SBA-15 having pore diameter from 2.4 to 14 nm using NMR. They have not seen any crystallization of benzene in MCM-41 and in

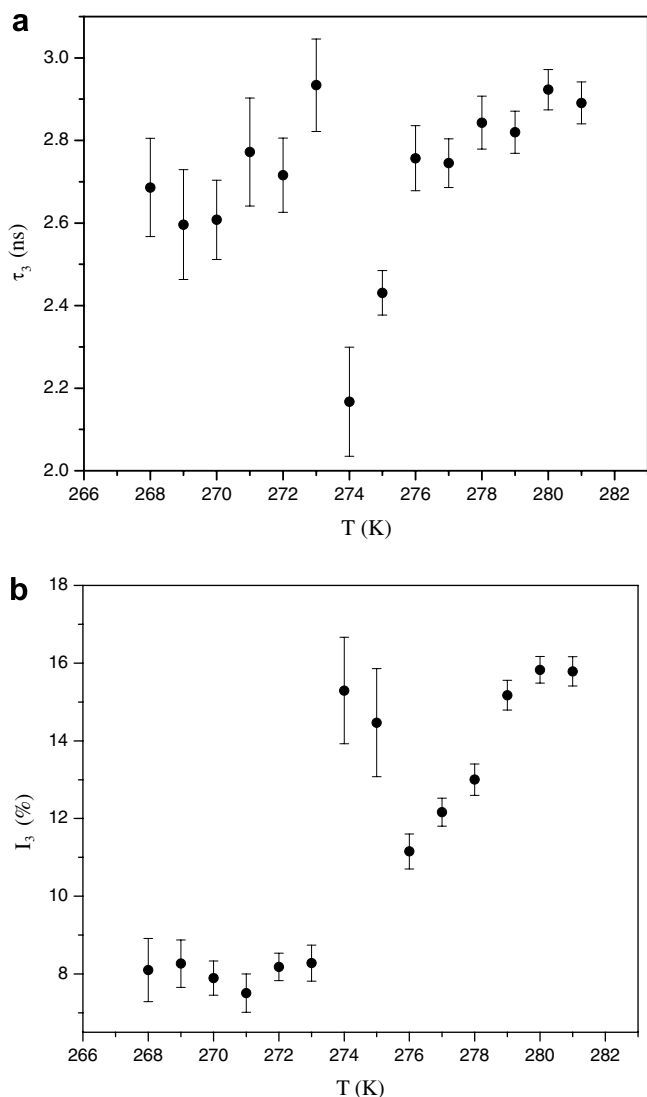


Fig. 3. Temperature dependence of *o*-Ps (a) pick-off lifetime ( $\tau_3$ ) and (b) pick-off intensity ( $I_3$ ) during cooling cycle.

the pores having diameter  $\leq 3.5$  nm for SBA-15, but observed glass to liquid like transition at the temperature range 170–175 K inside the pores of SBA-15. They have predicted that the minimum pore size required for crystallization of simple molecule like benzene having Van der Waals type interaction with the pore wall is roughly 10 molecular sizes. The same result was also obtained by Radhakrishnan et al. [10] through Monte Carlo simulation work considering the molecules to be confined in slit shaped pore with Lennard Jones potential. Bartkowiak et al. [8] has shown through grand canonical Monte Carlo simulation that a homogeneous crystalline confined phase results only for cylindrical pores with average diameter larger than 20 molecular sizes of the confined fluid. For cylindrical pores with diameters in the range 12–20 molecular sizes, an inhomogeneous phase with partially crystalline domains is formed and for cylindrical pores having diameter less than 12 molecular sizes, the confined phase

at low temperature consists of a hexatic phase in contact layer with amorphous inner region. In the present case, since the pore size is very small, the observations are expected to be due to partial crystalline phase of benzene molecule.

### 3.2. Reactivity of nitrobenzene

In order to study the effect of confinement on the reactivity of nitrobenzene towards Ps, different concentration of nitrobenzene in its mixture with benzene were incorporated to the pores of ZSM-5 and lifetime measurements were carried out at room temperature. Nitrobenzene was chosen because it is a known quencher of Ps. As mentioned earlier, when pure benzene is incorporated to ZSM-5, the  $\tau_4$  for *o*-Ps annihilation in meso pores disappears completely and the pick-off component ( $\tau_3$ ) of *o*-Ps reflects characteristic value of benzene although the obtained value of 2.8 ns is smaller than that seen in pure benzene (3.1 ns) [16]. The effect of nitrobenzene on the lifetime is shown in Table 2. Ps formation is completely quenched at nitrobenzene concentration  $\geq 0.55$  mMol. A dramatic increase in quenching rate or decrease in *o*-Ps lifetime ( $\tau_3$ ) with the increase in nitrobenzene concentration is observed as shown in Fig. 4. The expected change in lifetime at similar nitrobenzene concentration (in benzene) in liquid is also shown in Fig. 4 for comparison [24]. The quenching rate constant  $k$  is defined as  $\lambda_3 = \lambda_0 + k[C]$ , where  $\lambda_0$  is pick-off rate in pure benzene inside the pore,  $\lambda_3 (=1/\tau_3)$  is resultant annihilation rate in presence of nitrobenzene and  $C$  is its concentration. Fig. 4 shows that the *o*-Ps lifetime is very rapidly quenched with increase in the concentration ( $C$ ) of nitrobenzene and reaches a saturation value with  $C \geq 0.1$  mMol. The calculated reaction rate constant for nitrobenzene concentration  $\leq 0.1$  mMol is found to be  $\sim 40 \times 10^2 \text{ Mol}^{-1} \text{ ns}^{-1}$ , which is much larger than the reaction rate constant in bulk liquid ( $25.5 \text{ Mol}^{-1} \text{ ns}^{-1}$ ) [24]. This is the first observation of anomalous increase in Ps reaction rate inside the confined geometry. The larger value of reaction rate in confined geometry is qualitatively in agreement with the prediction through Monte Carlo simulation by Turner et al [25] in their study of chemical reaction kinetics on the basis of transition state theory of confined molecules inside Lennard Jones potential of slit shaped carbon pores.

Nitrobenzene, an electron acceptor and a known quencher of Ps, is known to form a complex with Ps atom. The reactivity is explained in terms of ‘bubble shrinkage rate’ ( $\sigma/2\eta$ , where  $\sigma$  is the surface tension and  $\eta$  is viscosity) and effect of ‘internal pressure’ due to surface tension [24]. Higher ‘internal pressure’ or higher surface tension is believed to increase the reactivity of Ps. This would mean an increase in surface tension of benzene and its mixtures in the confined geometry. This is also consistent with smaller bubble size in pure benzene in confined geometry. It is interesting to note that the surface energy of nanoparticles are significantly higher as compared to that of bulk mate-



Table 2

Positron annihilation lifetime for different concentration of nitrobenzene–benzene mixture incorporated in ZSM-5 zeolite

Mol fraction (%) of nitrobenzene	mMol concentration of nitrobenzene in 1 ml solution	Positron annihilation lifetime data					
		$\tau_1$ (ns)	$I_1$ (%)	$\tau_2$ (ns)	$I_2$ (%)	$\tau_3$ (ns)	$I_3$ (%)
0.01	0.001	0.17	18.27	0.60	79.98	2.61	2.18
0.1	0.01	0.20	32.46	0.41	64.14	2.39	2.87
1.0	0.11	0.19	33.46	0.42	64.10	2.18	2.59
2.0	0.22	0.20	29.31	0.39	68.28	2.15	2.40
5.0	0.55	0.17	19.74	0.36	79.87	–	–
10.0	1.10	0.23	35.23	0.39	64.61	–	–

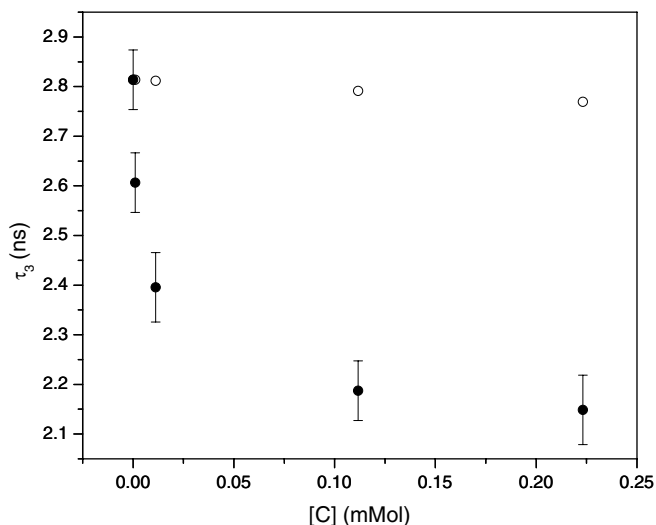


Fig. 4. Variation of *o*-Ps lifetime with the concentration of nitrobenzene in benzene. Closed circles (●) represent the quenching of *o*-Ps inside the pores, and open circles (○) represent the quenching of *o*-Ps in bulk (as calculated from [24]).

rial [26] and analogy can be drawn to confined liquids which have dimensionality in the same order. The saturation in quenching or the low reaction rate constant of *o*-Ps may be due to high viscosity at the higher concentration level of nitrobenzene. Despite the above-mentioned possibilities, the role played by the chemical nature of the surface cannot be ruled out. Further studies are required to understand the anomalous increase in Ps reaction rate.

#### 4. Conclusion

The phase transition behavior of benzene in confined geometry has been studied using positron annihilation spectroscopy. Two distinct domains of benzene, localized in micro and meso pores, are observed with characteristic freezing points, which are nearly 5–6 K and 2 K lower than the bulk value of 278.1 K. An anomalous increase in positronium reactivity in nitrobenzene–benzene mixture is seen. Although the possible reasons for anomalous increase in reactivity is discussed in terms of altered physical properties of the liquid in confinement, further studies are required to comprehend the exact nature the positronium interaction in confined geometry.

#### Acknowledgement

The authors thankfully acknowledge the help rendered by Dr. K.V. Chetty. Interesting discussions with Dr. A.K. Tripathi is also gratefully acknowledged.

#### References

- [1] C. Alba-Simionesco, B. Coasne, G. Dosseh, G. Dudziak, K.E. Gubbins, R. Radhakrishnan, M. Sliwinska-Bartkowiak, *J. Phys. Cond. Matt.* 18 (2006) R15.
- [2] N. Murase, K. Gonda, T. Watanabe, *J. Phys. Chem.* 90 (1986) 5420.
- [3] K.A. Jackson, B. Chalmers, *J. Appl. Phys.* 29 (1958) 1178.
- [4] R.F. Feldman, H. Cheng-yi, *Cement Concrete Res.* 15 (1985) 765.
- [5] C. Eyraud, J.F. Quinson, M. Brun, in: K. Unger, J. Rouquerol, K.S.W. Singh, H. Kral (Eds.), *Characterization of Porous Solids*, Elsevier, Amsterdam, 1988, p. 307.
- [6] C.L. Jackson, G.B. McKenna, *J. Chem. Phys.* 93 (1990) 9002.
- [7] G. Dossch, Y. Xia, C. Alba-Simionesco, *J. Phys. Chem. B* 107 (2003) 6445.
- [8] M. Sliwinska-Bartkowiak, G. Dudziak, R. Sikorski, R. Gras, R. Radhakrishnan, K.E. Gubbins, *J. Chem. Phys.* 114 (2001) 950.
- [9] M. Miyahara, K. Gubbins, *J. Chem. Phys.* 106 (1997) 2865.
- [10] R. Radhakrishnan, K.E. Gubbins, M. Sliwinska-Bartkowiak, *J. Chem. Phys.* 112 (2000) 11048.
- [11] J.A. Duffy, M.A. Alam, *Langmuir* 16 (2000) 9513.
- [12] J.A. Duffy, N.J. Wilkinson, H.M. Fretwell, M.A. Alam, *J. Phys. Cond. Matt.* 7 (1995) L27.
- [13] J.A. Duffy, N.J. Wilkinson, H.M. Fretwell, M.A. Alam, R. Evans, *J. Phys. Cond. Matt.* 7 (1995) L713.
- [14] M.A. Alam, A.P. Clarke, J.A. Duffy, *Langmuir* 16 (2000) 7551.
- [15] N.J. Wilkinson, M.A. Alam, J.M. Clayton, R. Evans, H.M. Fretwell, S.G. Usmar, *Phys. Rev. Lett.* 24 (1992) 3535.
- [16] H. Nakanishi, Y.C. Jean, in: D.M. Schrader, Y.C. Jean (Eds.), *Positron and Positronium Chemistry*, Elsevier, Amsterdam, 1988, pp. 159–192.
- [17] R.A. Ferrell, *Phys. Rev.* 108 (1957) 167.
- [18] D. Dutta, B. Ganguly, D. Gangopadhyay, T. Mukherjee, B. Dutta-Roy, *J. Phys. Cond. Matt.* 14 (2002) 7539.
- [19] D. Dutta, B. Ganguly, D. Gangopadhyay, T. Mukherjee, B. Dutta-Roy, *J. Phys. Chem. B* 108 (2004) 8947.
- [20] T.D. Dull, W.E. Frieze, D.W. Gidley, J.N. Sun, A.F. Yee, *J. Phys. Chem. B* 105 (2001) 4657.
- [21] D. Dutta, S. Chatterjee, B. Ganguly, K.T. Pillai, *J. Appl. Phys.* 98 (2005) 033509.
- [22] N.J. Turro, in: J. Klafter, J.M. Drake (Eds.), *Molecular Dynamics in Restricted Geometries*, John Wiley and Sons, New York, 1989, pp. 387–404.
- [23] P. Kirkegard, M. Eldrup, *Comp. Phys. Comm.* 17 (1991) 401.
- [24] Y. Kobayashi, Y. Ujihira, *J. Phys. Chem.* 85 (1981) 2455.
- [25] C.H. Turner, J.K. Brennan, J.K. Johnson, K.E. Gubbins, *J. Chem. Phys.* 116 (2002) 2138.
- [26] K.K. Nanda, A. Maisels, F.E. Kruis, H. Fissan, S. Stappert, *Phys. Rev. Lett.* 91 (2003) 106102.